

Reactor Performance and Safety Characteristics of ThN-UN Fuel Concepts in a PWR

Jacob P. Gorton^{1,2}, Benjamin S. Collins², Andrew T. Nelson², Nicholas R. Brown¹

¹University of Tennessee, Knoxville, TN 37916

²Oak Ridge National Laboratory, Oak Ridge, TN 37830

Abstract

The reactor performance and safety characteristics of mixed thorium mononitride (ThN) and uranium mononitride (UN) fuels in a pressurized water reactor (PWR) are investigated to discern the potential nonproliferation, waste, and accident tolerance benefits provided by this fuel form. This paper presents results from an initial screening of mixed ThN-UN fuels in normal PWR operating conditions and compares their reactor performance to UO₂ in terms of fuel cycle length, reactivity coefficients, and thermal safety margin. ThN has been shown to have a significantly greater thermal conductivity than UO₂ and UN. Admixture with a UN phase is required because thorium initially contains no fissile isotopes.

Results from this study show that ThN-UN mixtures exist that can match the cycle length of a UO₂-fueled reactor by using ²³⁵U enrichments greater than 5% but less than 20% in the UN phase. Reactivity coefficients were calculated for UO₂, UN, and ThN-UN mixtures, and it was found that the fuel temperature and moderator temperature coefficients of the nitride-based fuels fall within the acceptable limits specified by the AP1000 Design Control Document. Reduced soluble boron and control rod worth for these fuel forms indicates that the shutdown margin may not be sufficient, and design changes to the control systems may need to be considered. The neutronic impact of ¹⁵N enrichment on reactivity coefficients is also included. Due to the greatly enhanced thermal conductivity of the nitride-based fuels, the UN and ThN-UN fuels provide additional margin to fuel melting temperature relative to UO₂.

1. Introduction

Development of accident-tolerant fuel (ATF) materials for use in light water reactors (LWRs) has been emphasized by the Advanced Fuels Campaign (AFC) since the 2011 Fukushima accident. The purpose of the ATF program is to advance the technology readiness of fuel and cladding candidates that could enhance safety and performance of light water reactors (LWRs) during a severe accident without harming current reactor performance and safety characteristics. Among the ATF candidates considered in research and development efforts are composite fuels with uranium mononitride (UN) as one phase. UN fuel provides several

This manuscript has been authored by UT-Battelle, LLC, under contract DE-AC05-00OR22725 with the US Department of Energy (DOE). The US government retains and the publisher, by accepting the article for publication, acknowledges that the US government retains a nonexclusive, paid-up, irrevocable, worldwide license to publish or reproduce the published form of this manuscript, or allow others to do so, for US government purposes. DOE will provide public access to these results of federally sponsored research in accordance with the DOE Public Access Plan (<http://energy.gov/downloads/doe-public-access-plan>).

advantages over UO_2 , most notably a significantly higher thermal conductivity and higher uranium density. However, UN is known to chemically react and deteriorate in water, and has been shown to do so under water pressure and temperature representative of LWR operating conditions [1], [2], [3], [4]. To combat the reactivity of UN with water, research efforts have investigated the benefits of mixing UN with other fuel forms, such as UO_2 [5], [6] and another ATF candidate, U_3Si_2 , driven by the hypothesis that UO_2 or U_3Si_2 may shield UN from degradation in water [7], [4], [8].

Another potential fuel phase is thorium mononitride (ThN). The use of thorium in a thermal reactor presents several unique advantages and challenges compared to a traditional uranium-based fuel cycle. Thorium is approximately three times more abundant than uranium in Earth's crust [9], [10]. ^{233}U , produced from the absorption of a neutron by a ^{232}Th nucleus and subsequent β -decays, yields a greater reproduction factor, η , than ^{235}U or ^{239}Pu at thermal energies. This leads to better fuel cycle performance in terms of conversion ratio, and it opens the possibility of breeding or breakeven fuel cycles in a thermal reactor [9], [10], [11]. From a nonproliferation standpoint, the addition of thorium in an LWR leads to less plutonium production. The strong gamma emission from U-232 makes U-233 extraction a difficult process and therefore improves proliferation resistance [9], [12]. Additionally, thorium-fueled reactors could be used to reduce the plutonium stockpile since thorium systems initially require a neutron source to convert thorium into ^{233}U [11], [12].

Another benefit that most directly relates to the interests of the ATF program is that thorium-based fuels have a higher thermal conductivity than uranium-based fuels [9]. It has been shown that the thermal conductivity of ThO_2 is several times greater than that of UO_2 at low temperatures, but it approaches approximately the same value at elevated temperatures

(>1,200°C) [13], [14]. Further, transmutation of Th to Pa and U will degrade thermal conductivity during reactor operation [14], [15], [16], [17]. The thermal conductivity of ThN has also been shown to be greater than that of UN, and both ThN and UN have greater thermal conductivity than UO₂ [15]. Although the thermal conductivity of ThN decreases as the temperature increases, the opposite occurs for UN. Mixing the two fuels leads to a thermal conductivity that is an order of magnitude greater than that of UO₂ over the temperature range of interest for LWRs and up to at least 1,500°C. Higher thermal conductivity of the fuel pellets leads to a larger thermal safety margin in terms of the homologous temperature, which is the ratio of the maximum temperature in the fuel (i.e., the fuel centerline temperature) to the melting point of the fuel. The melting or disassociation point (temperature where solid mononitride transforms to liquid metal and gaseous nitrogen) of ThN and UN depends on the nitrogen overpressure, but is approximately 2,800–2,850°C when approximately atmospheric nitrogen pressure is available [2], [3], [18]. These temperatures are comparable to that of UO₂, which also melts at approximately 2,850°C [19]. Better thermal conductivity in nitride-based fuel forms may potentially reduce fission product release since the smaller temperature gradient in the fuel leads to smaller thermal stresses and a decreased likelihood of fuel pellet cracking [20].

A thorium-based fuel form also presents several challenges, the primary one being that thorium itself is not a fissile material and needs an external neutron source to convert thorium into the fissile ²³³U. Uranium can act as the external neutron source, but the ²³⁵U enrichment must be greater than the typical 5 wt% limit [12]. However, high assay, low-enriched uranium with enrichments greater than 5 but less than 20% may be used. Production of ²³³U from the β -decay of ²³³Pa, which is produced in the transmutation chain of ²³²Th and has a half-life of 27 days, can cause an increase in reactivity after a reactor has been shut down. Furthermore, the

^{232}U gamma that makes thorium fuels proliferation resistant also makes fuel refabrication difficult. Despite these challenges, thorium fuels have been used in high-temperature gas-cooled reactors (HTGRs) and water reactors, and concepts exist for their use in molten salt reactors (MSRs).

Bistructural- and tristructural-isotopic (BISO and TRISO) fuels using UO_2/ThO_2 fuel particles coated in pyrolytic carbon and silicon carbide layers have been used in the prototype HTGRs Peach Bottom 1 in the United States, AVR in Germany, and Dragon in the UK. After successful experiments in these reactors, thorium fuels were used in the Fort Saint Vrain and Thorium High Temperature Reactor (THTR) experimental reactors in the United States and Germany, respectively [11], [21]. The successful Molten Salt Reactor Experiment (MSRE) at the Oak Ridge National Laboratory (ORNL) led to the development of the Molten Salt Breeder Reactor (MSBR) project, which utilized a thorium fuel cycle [22]. More recently, fast-spectrum, thorium-fueled MSR concepts are being revisited [23].

Mixed UO_2/ThO_2 fuels were used in the Elk River and Indian Point LWRs [11], and the Shippingport reactor made use of the seed-blanket concept [24] to demonstrate breeding in an LWR. The seed-blanket concept, also known as the Radkowsy Thorium Fuel (RTF) concept [25], uses fissile seed regions to initially fuel the reactor and to supply neutrons to the blanket region of thorium, which is transmuted into ^{233}U for continued operation. LWRs with reduced moderation have been proposed, including heavy water PWRs and tight-pitch BWRs, both of which have a smaller moderator-to-fuel ratio and larger conversion ratio than typical LWRs, and they primarily operate in an intermediate energy spectrum (1 eV to 100 keV). Evaluations of these concepts show that break-even or breeding can be achieved in these systems when seed-blanket concepts and reduced moderator-to-fuel ratios are used [26], [27], [28].

This paper presents a preliminary analysis of homogenously mixed ThN-UN fuels in a typical PWR pin cell. The Consortium for Advanced Simulation of Light Water Reactors (CASL) deterministic reactor physics code MPACT [29] was used to determine ThN/UN mixture ratios and corresponding ^{235}U enrichments needed to match the cycle length of typical UO_2 fuel. To enhance confidence in the results, these cycle length calculations were compared with results from the Monte Carlo code Serpent [30]. Fuel temperature (or Doppler) and moderator temperature coefficients, as well as soluble boron and control rod worth, were determined using MPACT. The impact of 100% enriched ^{15}N in the ThN and UN phases on the ^{235}U enrichment required to meet the UO_2 cycle length and reactivity coefficients is investigated. Finally, a thermal hydraulic performance comparison in terms of homologous temperature is made between the ThN/UN mixtures and the UO_2 baseline using the coupled neutronics and thermal hydraulics capabilities of MPACT and CTF [31] within CASL's Virtual Environment for Reactor Application – Core Simulator (VERA-CS).

2. 2-D Pin Cell Description and ThN-UN Mixture Determination

2.1 Model Descriptions

2-D PWR pin cell models were developed in MPACT to determine the combinations of ThN-UN and ^{235}U enrichments needed to match the cycle length of a pin cell with 4.90% enriched UO_2 using a 252-group ENDF/B-VII.1 nuclear cross section library [32]. The P2 approximation was used for scattering, and all models treated the ^{232}Th and ^{238}U resonances explicitly rather than lumping them together. MPACT was chosen as the primary tool for this analysis due to its speed as a deterministic code, its LWR-focused development, and its ease of coupling to the thermal hydraulic subchannel code CTF within CASL's VERA-CS. Zircaloy-4

cladding and a helium pellet-cladding gap were used in the pin cell models. The geometry used is based on the AP1000 design [33], and reflective boundary conditions were applied on all sides of the model. A fuel temperature of 900 K was used, and all other temperatures in the model were set to the AP1000 inlet temperature of 552.6 K (535.0°F). The same power density in W/cm³ was used in all models and is also equal to that of the AP1000.

2.2 UO₂ Cycle Length Matching

The ²³⁵U enrichment required to meet the UO₂ cycle length was determined for a 100% UN case, a 20% (by weight) ThN-80% UN mixture, and a 40% ThN-60% UN mixture. Additionally, a mixture with maximized thorium content was determined by setting the ²³⁵U enrichment to 19.90% and adjusting the ThN and UN weight fractions (which also changes the density of the mixture) until the UO₂ fuel cycle was met. Fuel cycle lengths were calculated using the linear reactivity model [34], assuming a three-batch fuel management scheme and 3% neutron leakage. The UO₂ cycle length was calculated to be 472 effective full power days (EFPDs), and the nitride-based fuel compositions were accepted if their cycle lengths matched this target value within 3%. The density of UN and ThN can be found in a forthcoming paper by Parker et al. [15], where theoretical densities of 95% and 92% were used for UN and ThN, respectively. Equation (1) was used to calculate the density of the mixtures, where x_i refers to the weight fraction of each constituent in the mixture.

$$\rho_{mix} = \sum_{i=1}^n x_i \rho_i \quad (1)$$

The nitride-based fuel compositions found to match the UO₂ cycle length are listed in Table 1, which also lists the three-batch discharge burnup of the fuels, all of which are lower

than the calculated UO_2 discharge burnup of 56.06 GWd/t. Discharge burnup is lower for the UN and ThN-UN fuels because of their greater heavy metal loading (due to increased density) and increased absorption from ^{232}Th , ^{238}U , and ^{14}N . These mixtures were determined using natural nitrogen, which is more than 99% ^{14}N . UN fuels have been considered which are enriched to 90% ^{15}N or more because of its smaller absorption cross section in the thermal region compared to ^{14}N [4], [35], but doing so increases production costs, and natural nitrogen is the current default in the VERA-CS modeling suite. ^{15}N enrichment is also preferable because of the (n,p) reaction that occurs in ^{14}N , which produces the radioactive ^{14}C and poses a disposal issue. Brown, Todosow, and Cuadra [6] consider the neutronic penalty caused by using natural nitrogen rather than ^{15}N enrichment. Section 4 of this article recalculates the ^{235}U enrichments needed to match the UO_2 cycle length for 20% ThN-80% UN, 40% ThN-60% UN, and UN cases, as well as the maximum possible weight fraction of ThN for a ^{235}U enrichment of 19.90% using 100% enriched ^{15}N .

Table 1: ThN-UN mixtures that approximately match the UO_2 cycle length

Thorium Content (wt%)	UN content (wt%)	^{235}U Enrichment (wt%)	Cycle Length (EFPD)	Discharge Burnup (GWd/t)
20.0	80.0	7.80	471	41.81
40.0	60.0	11.10	472	43.68
66.0	34.0	19.90	469	45.99
0	100	5.20	470	38.04

2.3 Verification with Serpent and Flux Spectra Characterization

Because MPACT is a deterministic code optimized for LWR analysis and traditional UO_2 fuel, the predictions of k-effective as a function of burnup for the ThN-UN mixtures are compared to predictions by the Monte Carlo code Serpent for verification. Figure 1 shows a comparison of the three-batch, 3% neutron leakage k-effective throughout the cycle as predicted by MPACT and Serpent, as well as the absolute difference between the two codes in pcm for the UO_2 , UN, and all ThN-UN mixtures. At beginning of life (BOL), the difference in k-effective between the two codes is 100–500 pcm for all cases. Brown et al. (2014) [4] show that differences in k-effective calculated by Serpent and TRITON for UN fuels of varying densities at BOL were between 290 and 327 pcm when a 238-group cross section library was used in TRITON. Serpent predicted a greater k-effective at BOL but a smaller k-effective at end of life (EOL) for all cases. Note that the Serpent continuous energy library is based on the ENDF/B-VII.0 data library [36], whereas the MPACT models used ENDF/B-VII.1 data, which may explain some of the differences between predictions from the two codes. The behavior trends between the two codes were consistent across each enrichment and fuel type considered.

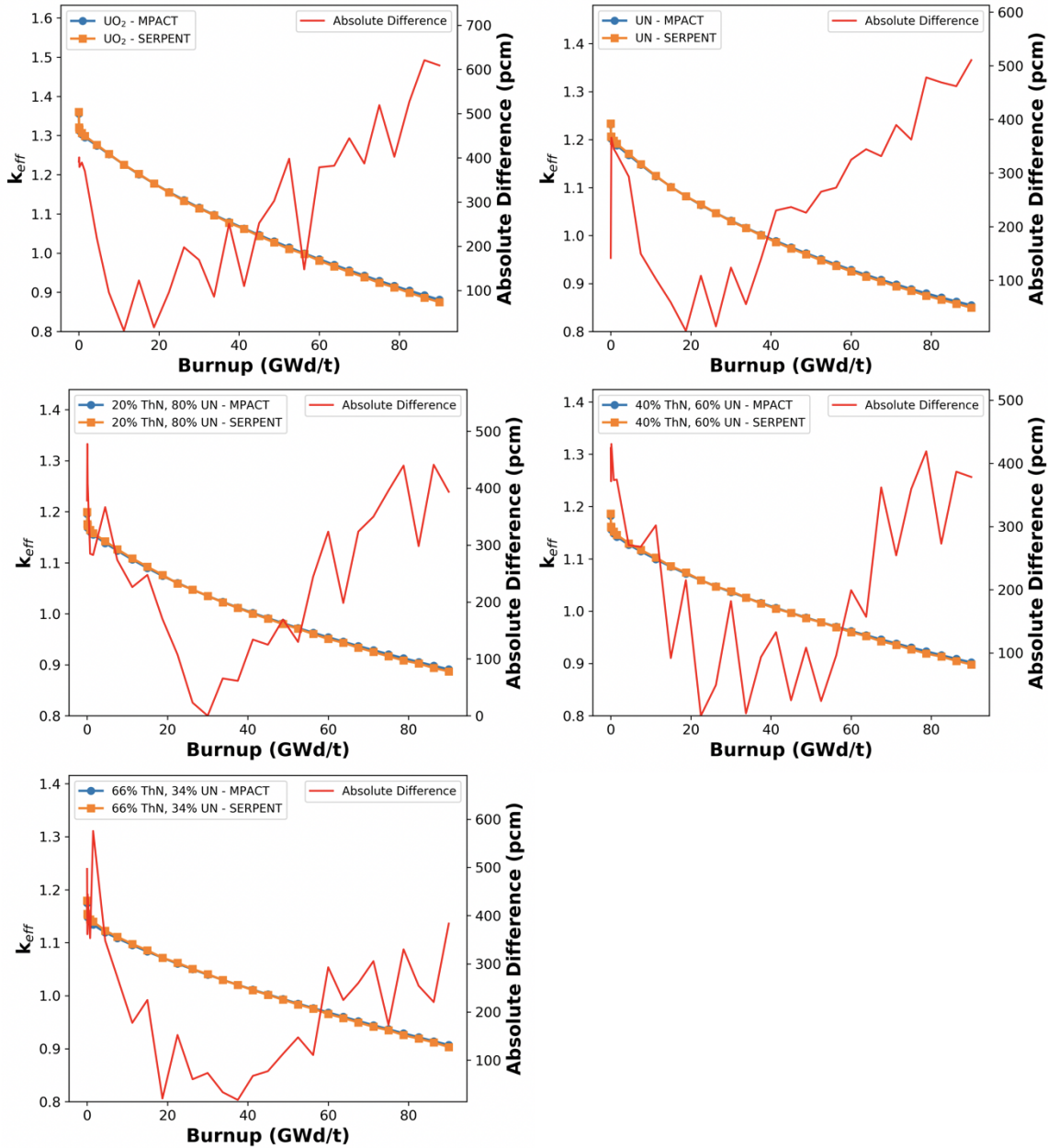


Figure 1: Comparison of k-effective calculated by MPACT and Serpent

A comparison of the ^{232}Th and ^{233}U mass throughout the cycle calculated by MPACT and Serpent is shown in Figure 2. The relative difference in mass calculations between MPACT and Serpent is less than 1.2% for ^{233}U and less than approximately 0.03% for ^{232}Th across all burnup steps.

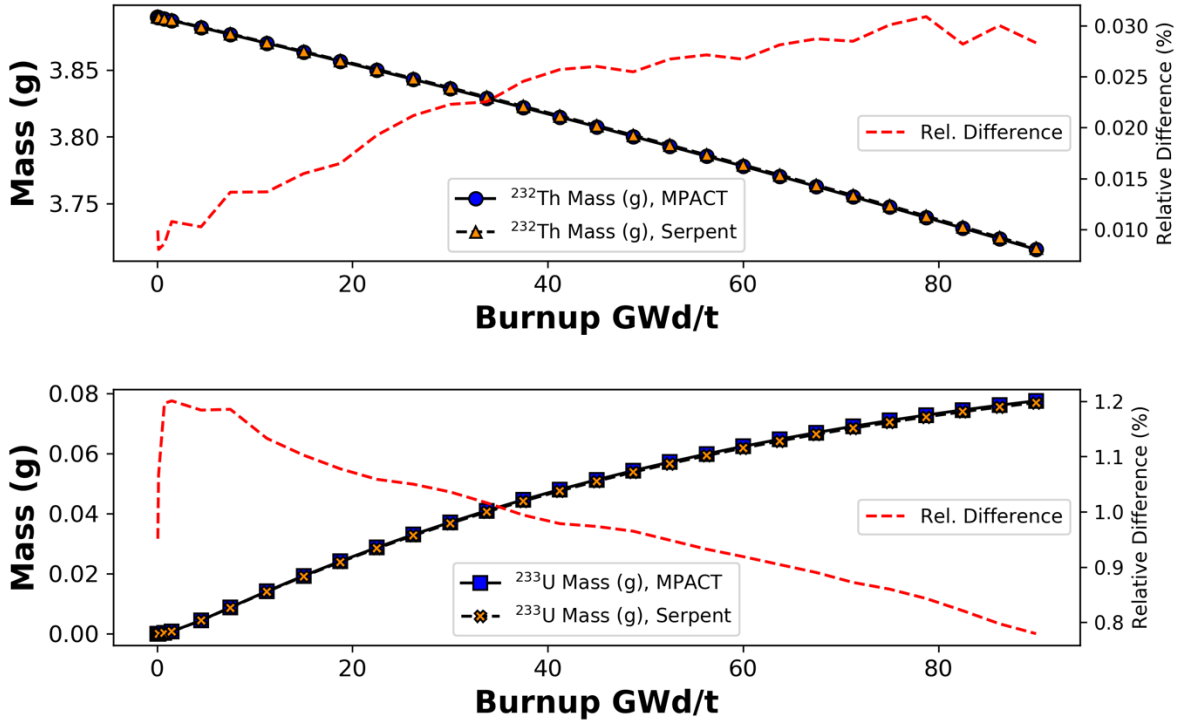


Figure 2: Comparison of ^{232}Th and ^{233}U mass as a function of burnup in the 66% ThN, 34% UN mixture

Normalized neutron flux spectra at BOL calculated using MPACT are shown in Figure 3 for the thermal and intermediate energy regime and in Figure 4 for the fast energy regime. All spectra are typical of a thermal LWR, but UN has a harder spectrum than UO_2 due to the greater amount of ^{238}U , and the ThN-UN fuels have an even harder spectrum than UN because of the presence of thorium. However, the neutron spectrum is softer for the ThN-UN mixed fuels at EOL compared to UN due to the build-up of ^{233}U throughout the cycle. This is shown in Figure 5, where the BOL and EOL thermal and intermediate flux spectra are shown for UO_2 , UN, and 66ThN-34UN.

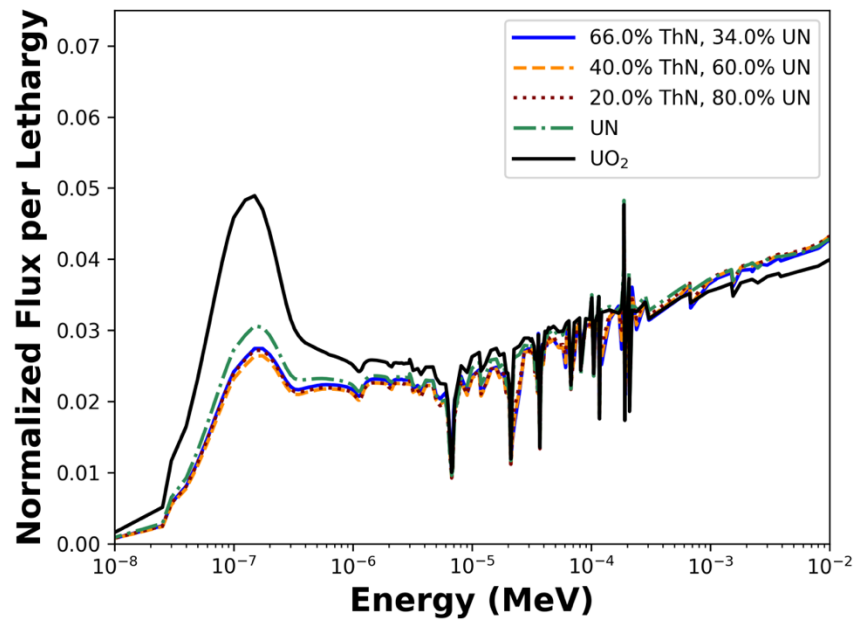


Figure 3: Thermal and intermediate neutron flux spectra for UO_2 , UN , and ThN-UN mixtures

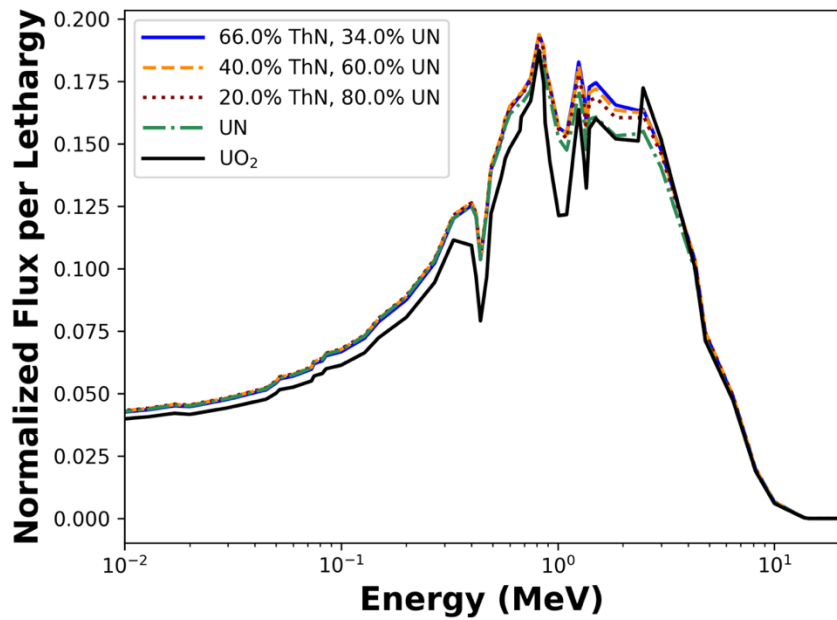


Figure 4: Fast neutron flux spectra for UO_2 , UN , and ThN-UN mixtures

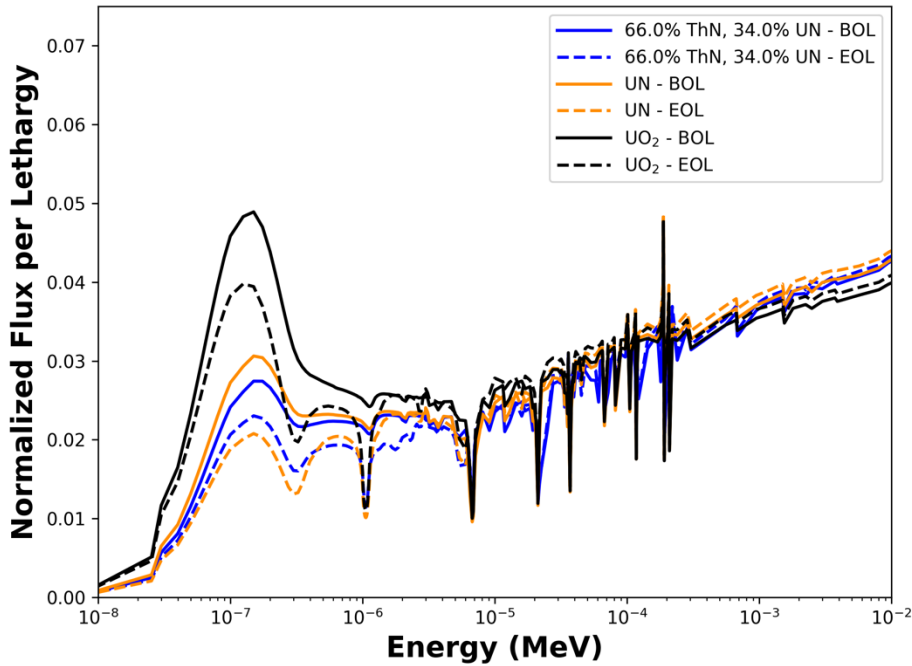


Figure 5: Comparison of BOL and EOL thermal and intermediate flux spectra for UO_2 , UN, and 66ThN-34UN

3. Fuel Performance Comparison

3.1 Reactivity Coefficients

MPACT was used to calculate the fuel temperature (or Doppler) and moderator temperature coefficients, as well as the boron coefficient and control rod worth, for each of the ThN-UN mixtures listed in Table 1. These calculations were performed as a function of burnup and compared to the UO_2 reactivity coefficients. The Doppler coefficient is shown in Figure 6, and the moderator temperature coefficient is shown in Figure 7. Figure 8 shows the impact of boron concentration on the moderator temperature coefficient for the UO_2 and 66ThN-34UN cases using soluble boron concentrations of 0, 500, and 1,000 ppm. The soluble boron coefficient is shown in Figure 9 and was calculated using boron concentrations of 0 and 1,000 ppm at each burnup step. The pin cell model described in Section 2 was used to calculate the Doppler,

moderator temperature, and boron coefficients. To calculate the control rod worth shown in Figure 10, a 2D quarter-symmetry 17×17 fuel assembly model with silver-indium-cadmium (Ag-In-Cd) control rods was used.

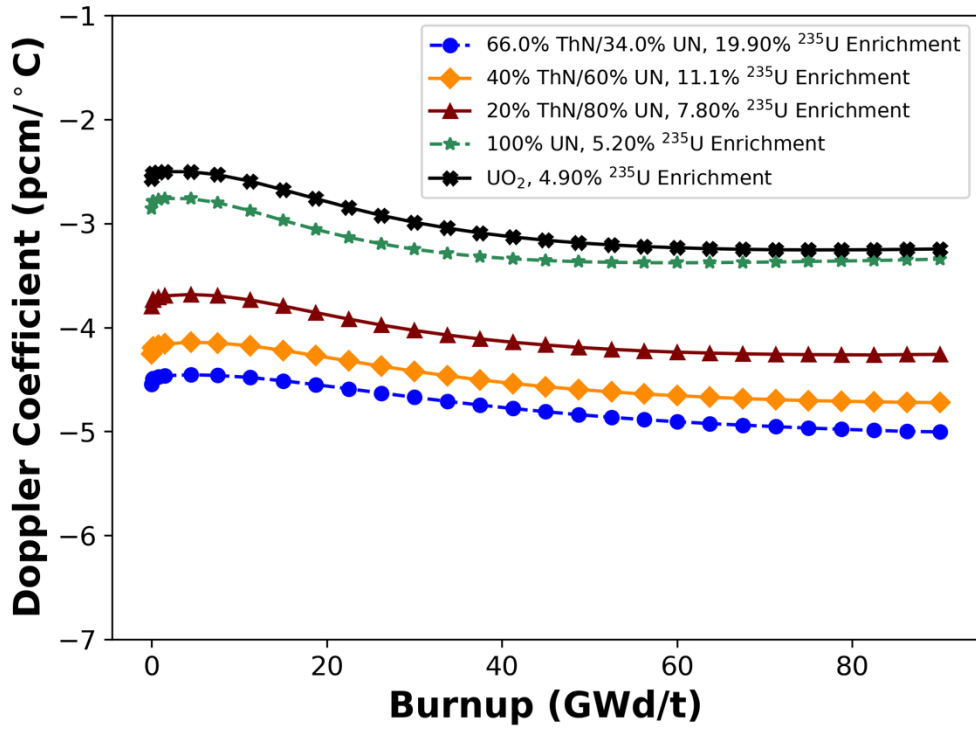


Figure 6: Doppler coefficient of UO₂, UN, and ThN-UN fuels as a function of burnup

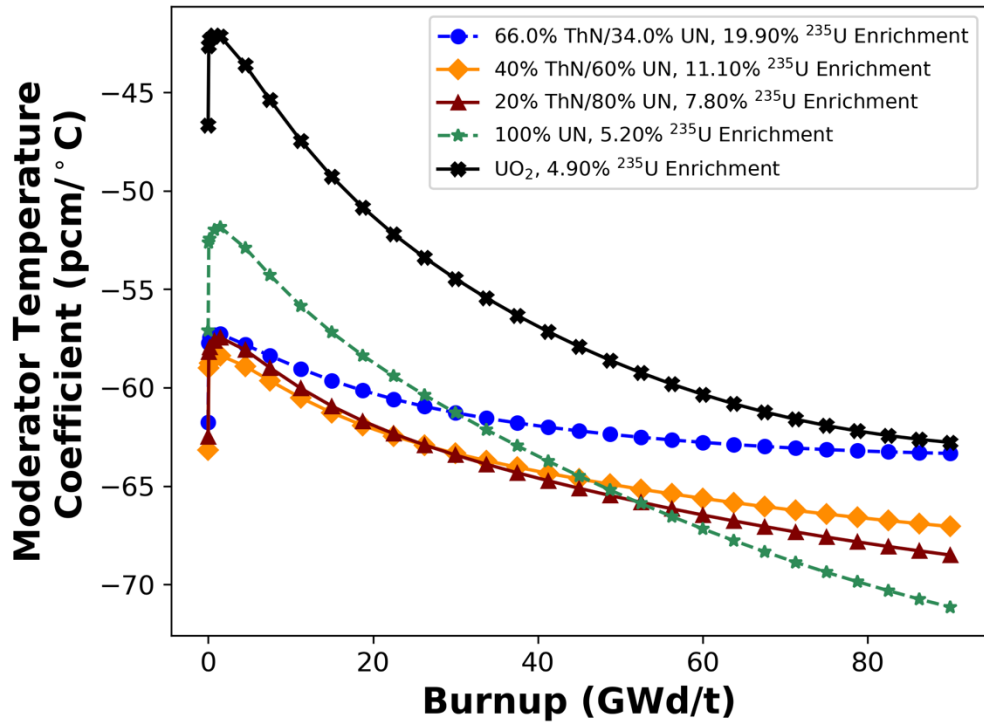


Figure 7: Moderator temperature coefficient of UO_2 , UN, and ThN-UN fuels as a function of burnup

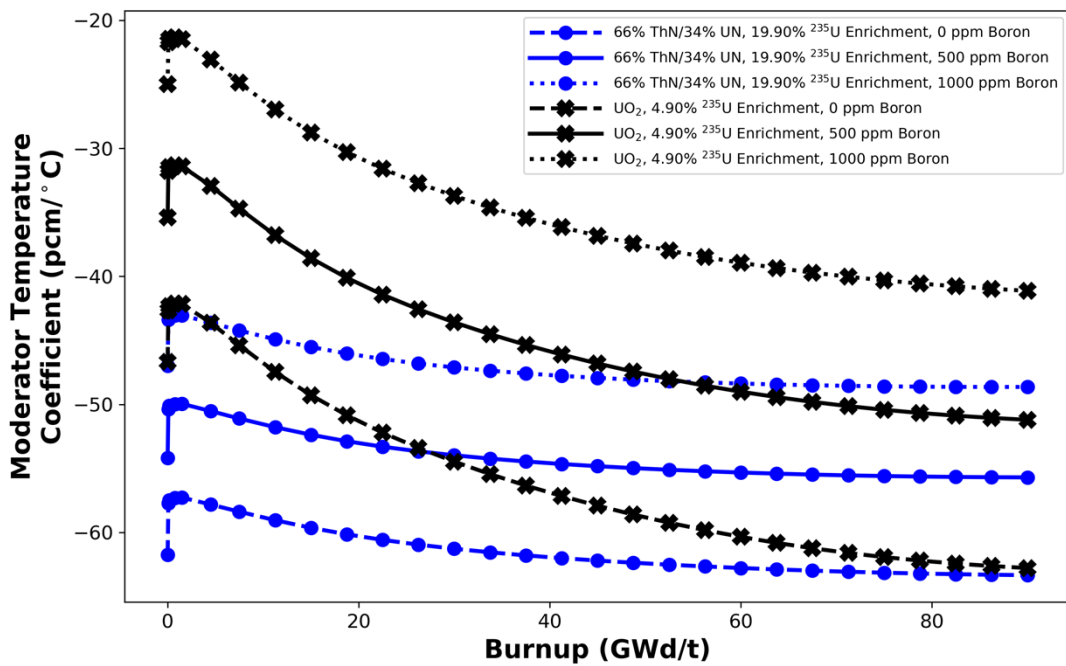


Figure 8: Impact of boron on moderator temperature coefficient for UO_2 and 66ThN-34UN

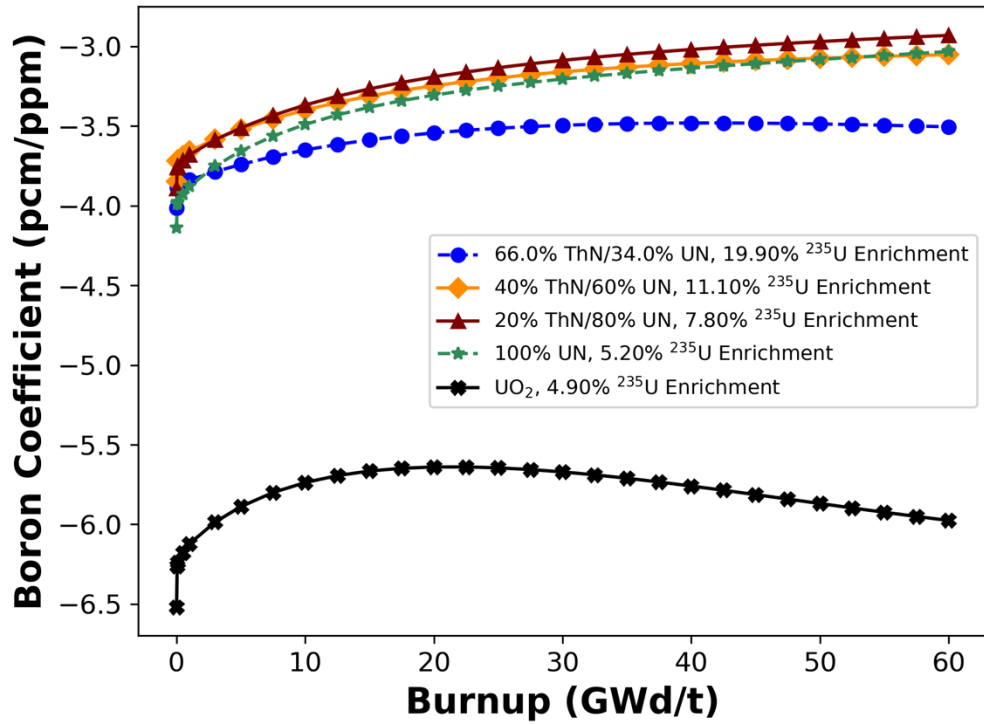


Figure 9: Soluble boron coefficient of UO_2 , UN, and ThN-UN fuels as a function of burnup

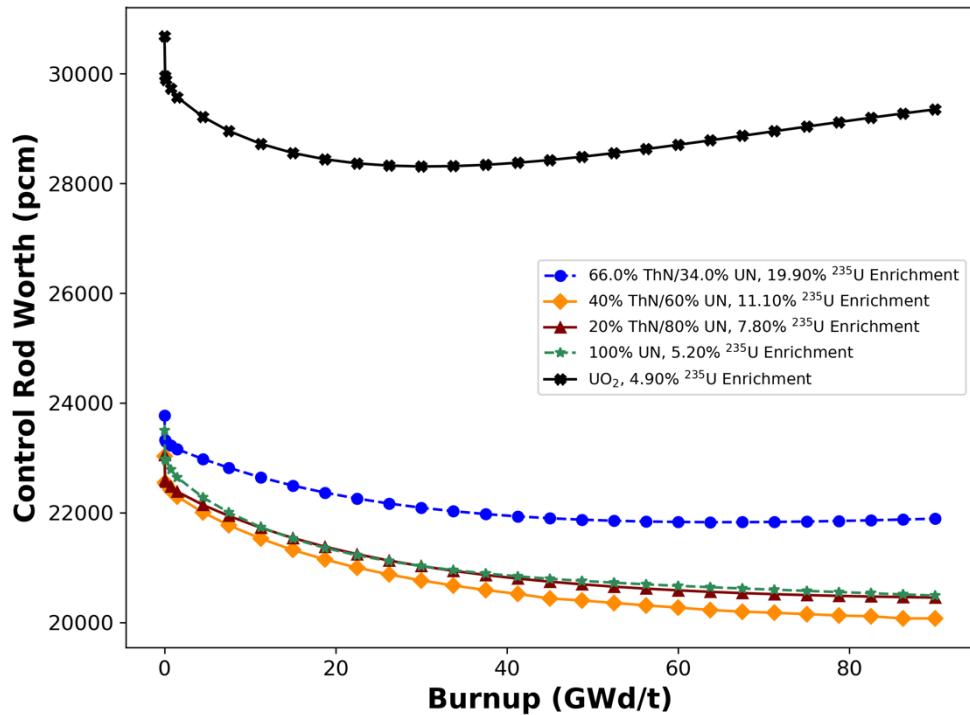


Figure 10: Control rod worth of UO_2 , UN, and ThN-UN fuels as a function of burnup

Greater fuel density, increased parasitic absorption, reaction yields (e.g. ^{233}U production), and evolution of the isotopes with burnup are all factors in explaining why the reactivity coefficients and control worth for the nitride fuel forms differ from UO_2 . The Doppler coefficient for the nitride-based fuels is more negative than for UO_2 because of the greater fuel density and increased resonance absorption from ^{238}U and ^{232}Th . Increased heavy metal loading in the UN and ThN-UN cases reduces the moderator-to-fuel ratio and enhances under-moderation. This is the primary cause of the more negative moderator temperature coefficient for the nitride cases compared to the UO_2 case. Production of ^{233}U throughout the cycle and differences in BOL and EOL cross sections cause the ThN-UN mixtures to have a less negative moderator temperature coefficient at EOL compared to UN. For example, at BOL, the 66% ThN-34% UN case has the largest thermal capture cross section and UN has the smallest out of the nitride-based fuels, but the opposite is true at EOL.

Increased absorption causes the nitride-based fuels to have lower control rod and soluble boron worth than UO_2 . ^{233}U production and cross section evolution dictate the change in control worth with burnup for each nitride fuel. Additionally, each fuel type considered has a different equilibrium ^{135}Xe concentration, which impacts the amount of parasitic absorption in the fuel and therefore impacts the reactivity coefficients and control worth. To further illustrate these points, the BOL and EOL two-group macroscopic capture cross sections (Σ_c) for each fuel type are shown in Table 2, and the mass of ^{135}Xe in each pin cell model as a function of burnup is shown in Figure 11.

Table 2: Two-group macroscopic capture cross sections for each fuel form at BOL and EOL

	Fast Energy Σ_c (cm $^{-1}$)		Thermal Energy Σ_c (cm $^{-1}$)	
	BOL	EOL	BOL	EOL
UO ₂	0.0223	0.0306	0.0837	0.1936
UN	0.0310	0.0389	0.1476	0.3348
20% ThN – 80% UN	0.0325	0.0396	0.1587	0.3228
40% ThN – 60% UN	0.0322	0.0389	0.1684	0.3073
66% ThN – 34% UN	0.0306	0.0366	0.1755	0.2735

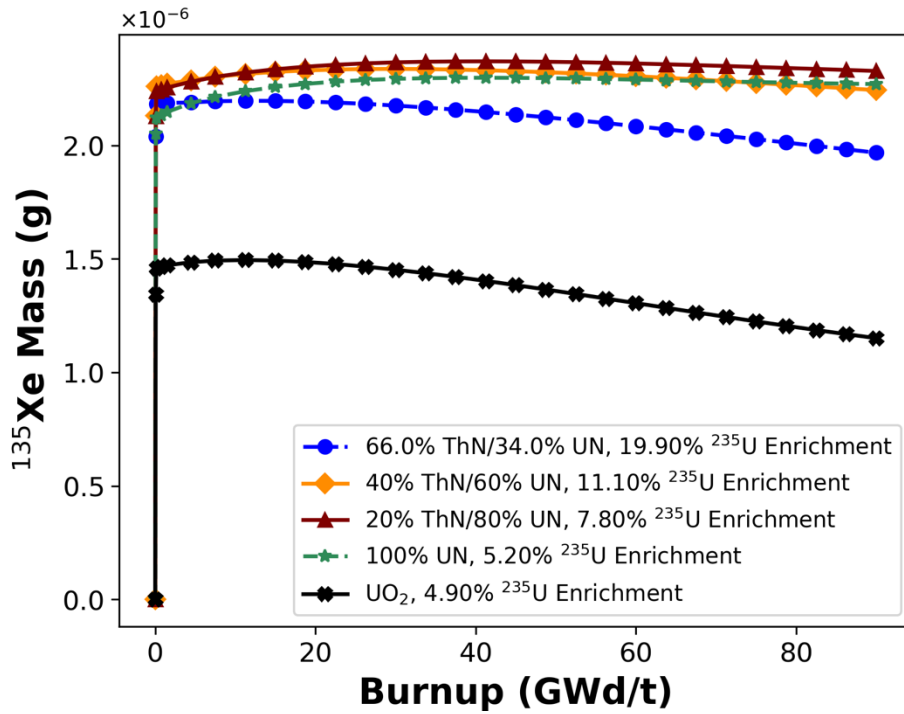


Figure 11: ^{135}Xe mass as a function of burnup for each fuel form

Table 3 lists the ranges of reactivity coefficients for each fuel type found in this study and compares them to the limits specified in the AP1000 Design Control Document (DCD) [33]. Note that the AP1000 DCD limits take into account a range of fuel and moderator temperatures across varying operating conditions, whereas only 900 K and 800 K were used as fuel

temperatures and 550 K and 585 K were used as moderator temperatures in this study. The moderator temperature coefficients listed from this study are at 0 boron concentration.

Table 3: Comparison of reactivity coefficients to AP1000 DCD limits

Case	Doppler Coefficient (pcm/°C)	Moderator Temperature Coefficient (pcm/°C)	Boron Coefficient (pcm/ppm)
AP1000 DCD	-6.3 to -1.8	-72 to 0	-13.5 to -5.0
UO ₂	-3.3 to -2.5	-62.8 to -42.1	-6.5 to -5.6
UN	-3.4 to -2.8	-71.1 to -51.9	-4.1 to -3.0
20% ThN – 80% UN	-4.3 to -3.7	-68.5 to -57.5	-3.9 to -2.9
40% ThN – 60% UN	-4.7 to -4.1	-67.1 to -58.4	-3.8 to -3.1
66% ThN – 34% UN	-5.0 to -4.5	-63.3 to -57.3	-4.0 to -3.5

All Doppler and moderator temperature coefficients calculated in this study fall within the AP1000 DCD limits, but the boron coefficients for UN and the ThN-UN mixtures are less negative than the specified limits. The larger absolute values of the UN and ThN-UN moderator temperature coefficients, along with the significantly lower control rod worth for these fuels shown in Figure 10, may pose an issue with shutdown margin. Typically, a shutdown margin of 1.0–1.3% is required under all reactor conditions, the most limiting of which occur at cold moderator temperatures such as cold zero power or during a main steam line break in a PWR. In their analysis of a Th-MOX-fueled PWR core, Fridman and Kliem [37] also predicted a reduced boron worth and control rod worth in the Th-based fuels compared to a UO₂ baseline. They addressed this problem by suggesting that the soluble boron be enriched to 40% ¹⁰B and by replacing Ag-In-Cd control rods with more absorbing B₄C control rods. The nitride-based fuels have less excess reactivity, as shown in Figure 1, which may help compensate for the lower

boron and control rod worth, but similar design changes may be required for a ThN-UN-fueled reactor.

3.2 Thermal Performance

A 3D fuel pin model was developed to evaluate the thermal performance of ThN-UN fuels relative to UO_2 . The model utilizes VERA-CS's thermal–hydraulics–to–neutronics coupling capability between CTF and MPACT. The fuel pin design is based on the AP1000 design, with the power and coolant mass flow rate scaled for a single pin and four surrounding subchannels. The same power density in W/cm^3 was used for all fuel forms. CTF's dynamic gap conductance model was employed. The thermal conductivity and heat capacity for ThN and UN found in the forthcoming paper by Parker et al. [13] were used, and the thermal properties for the ThN-UN mixtures were estimated for calculation purposes using the respective volume fractions of each phase. The thermal conductivity and specific heat capacity of UN, ThN, and the ThN-UN mixtures used in the CTF models are shown in Figure 12 and Figure 13, respectively.

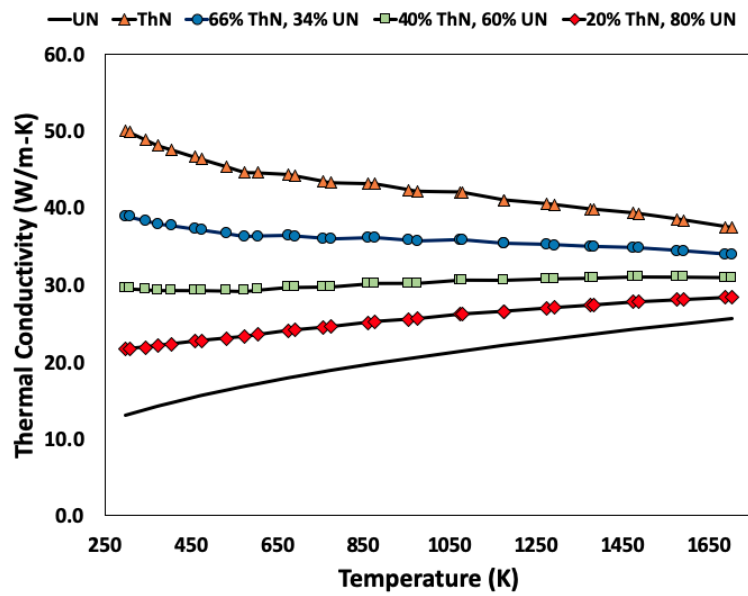


Figure 12: Thermal conductivity of UN, ThN, and ThN-UN mixtures

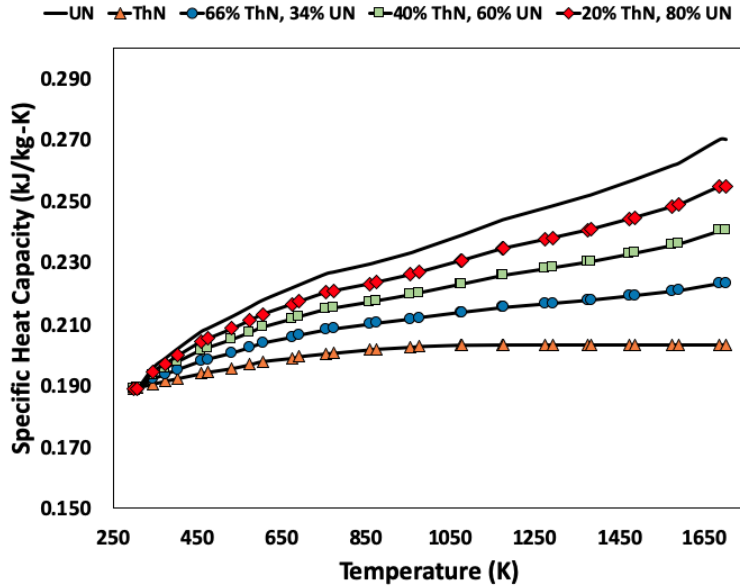


Figure 13: Specific heat capacity of UN, ThN, and ThN-UN mixtures

Figure 14 presents the calculated axial dependence of homologous temperature in the fuel pin for the different fuel forms at BOL, and the maximum homologous temperature as a function of burnup for each fuel form is shown in Figure 15. The homologous temperature is the ratio of the maximum fuel temperature (fuel centerline temperature) to the melting (or disassociation) temperature of the fuel. For UO_2 and 100% UN, a melting temperature of 2,850°C was used, and for the ThN mixtures, a melting temperature of 2,790°C was used.

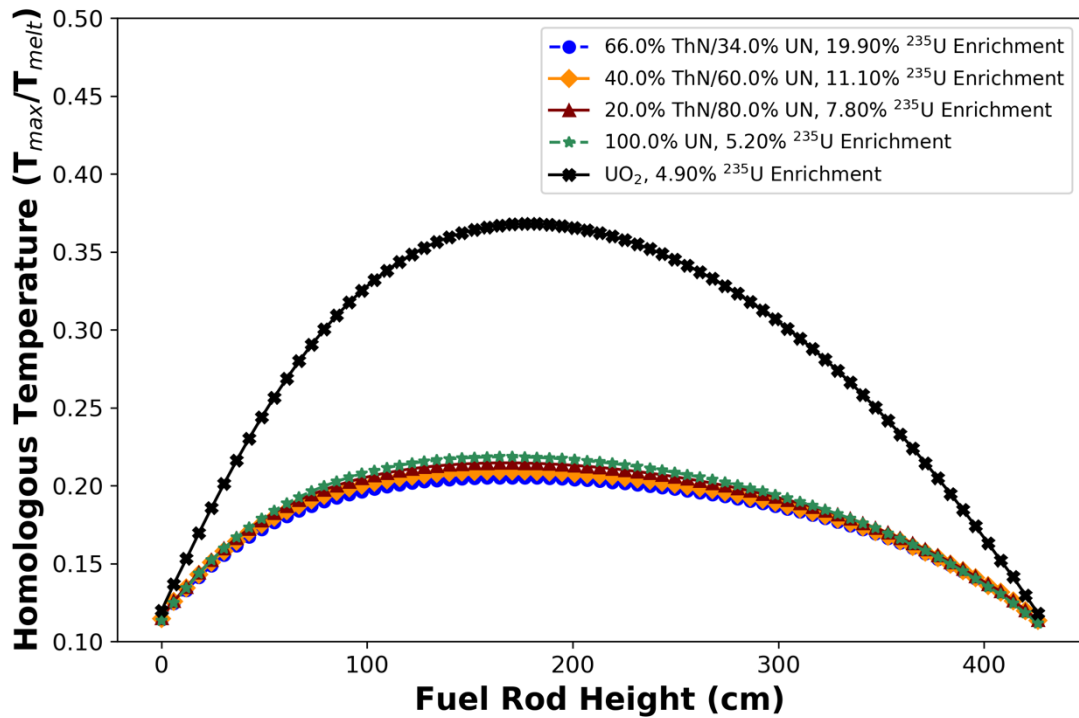


Figure 14: Homologous temperature as a function of fuel rod height at BOL

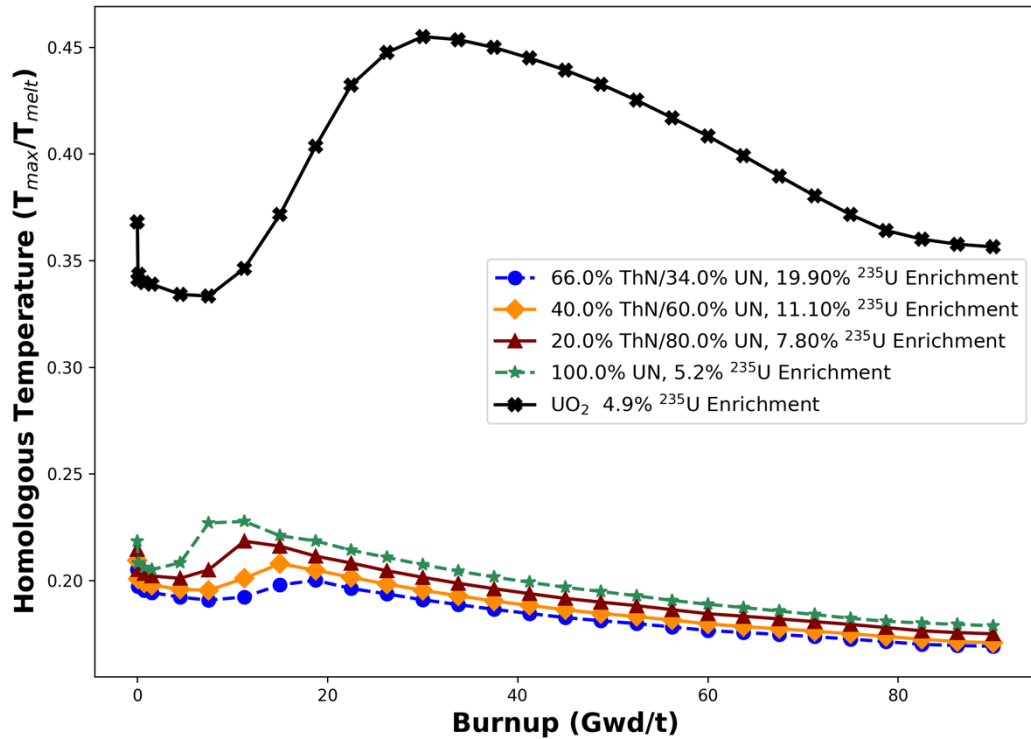


Figure 15: Homologous temperature as a function of burnup

The maximum homologous temperature reached at BOL was 0.37 for UO_2 , and it was between 0.20 and 0.22 for all UN and ThN-UN cases. As a function of burnup, the homologous temperature for UO_2 peaks at approximately 0.45, but never gets above 0.23 for UN or any ThN-UN mixture. The change in homologous temperature as a function of burnup is caused by the shifting relative power profile in the rod. Note that the same thermal properties for fuel were used at all burnup steps. The significantly lower homologous temperature obtained using UN and ThN-UN fuels illustrates the enhanced thermal safety margin and accident tolerance of nitride-based fuels over oxide fuels. Although this calculation was performed under normal operating conditions, the nitride-based fuels may also have an improved safety margin during an accident scenario, thus reducing the likelihood of fuel melting and fission product release. An additional benefit from the greater thermal conductivity and smaller axial temperature gradient shown in Figure 14 is that there will be smaller thermal stresses induced in the fuel pellets and cladding, which may reduce the likelihood of pellet cracking and fission product release.

4. Impact of 100% Enriched ^{15}N

All results presented thus far in the study used natural nitrogen, which is primarily ^{14}N , in UN and ThN phases. Previous studies have shown that ^{15}N enrichment boosts reactor and fuel performance over natural nitrogen since ^{14}N is a significant neutron absorber at thermal energies [4], [8], [35]. The differences in fuel performance from using 100% enriched ^{15}N in UN and ThN-UN fuels in terms of required ^{235}U enrichment and reactivity coefficients are quantified in this section.

The ^{235}U enrichments required to approximately match the 4.90% enriched UO_2 cycle length of 472 EFPDs are listed in Table 4.

Table 4: ThN-UN mixtures with enriched ^{15}N that approximately match the UO_2 cycle length

Thorium Content (wt%)	UN Content (wt%)	^{235}U Enrichment (wt%)	Cycle Length (EFPD)
20.0	80.0	5.90	475
40.0	60.0	8.50	478
73.5	26.5	19.90	480
0	100	3.90	478

For 100% ^{15}N enriched 20% ThN-80% UN, 40% ThN-60% UN, and UN, the relative decrease in required ^{235}U enrichment from the natural nitrogen cases are 24.4%, 23.4% and 25%, respectively. The maximum possible thorium content increased from 66 wt% to 73.5 wt%, a relative increase of 11.4%.

To illustrate the impact of ^{15}N enrichment on reactivity coefficients, the 40% ThN-60% UN mixture is considered. Figure 16 shows the Doppler coefficient as a function of burnup for 40% ThN-60% UN with natural nitrogen and 100% enriched ^{15}N , as well as the UO_2 reference case. Similar comparisons are shown in Figure 17–Figure 19 for moderator temperature coefficient, soluble boron coefficient, and control rod worth, respectively.

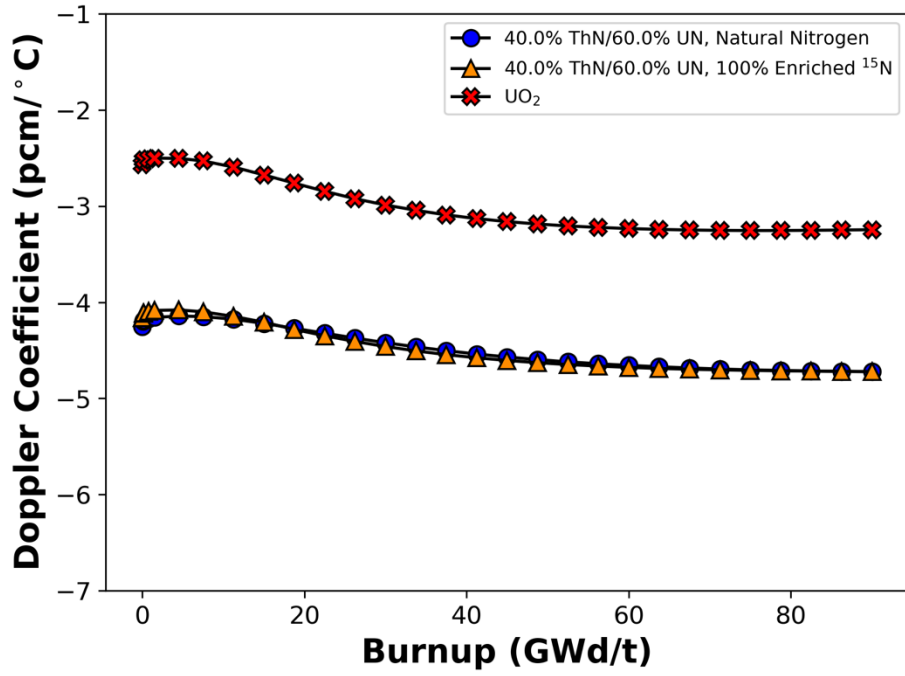


Figure 16: Doppler coefficient for UO₂, 40ThN-60UN with natural nitrogen and 40ThN-60UN with 100% ¹⁵N enrichment

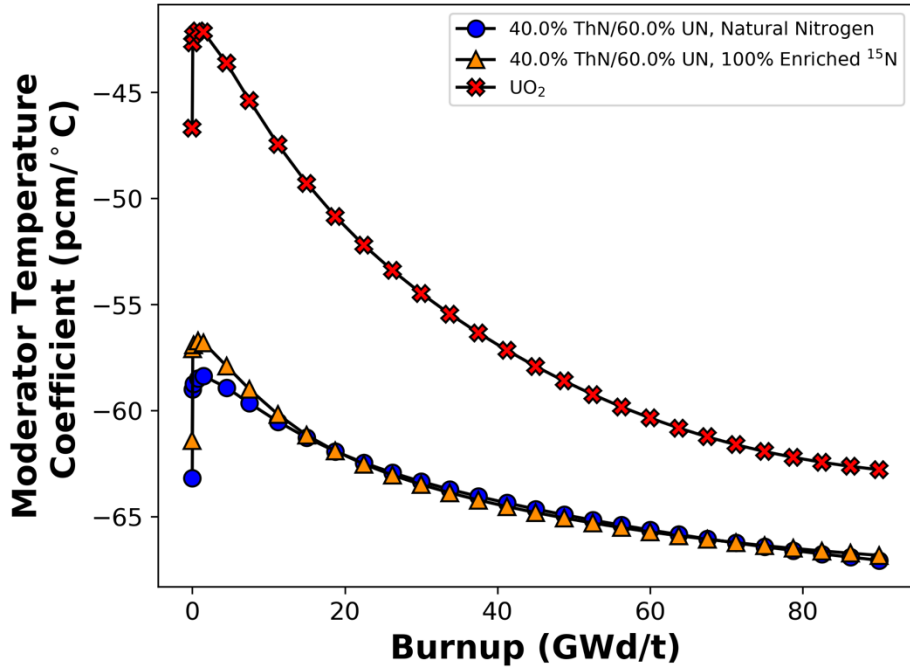


Figure 17: Moderator temperature coefficient for UO₂, 40ThN-60UN with natural nitrogen, and 40ThN-60UN with 100% ¹⁵N enrichment

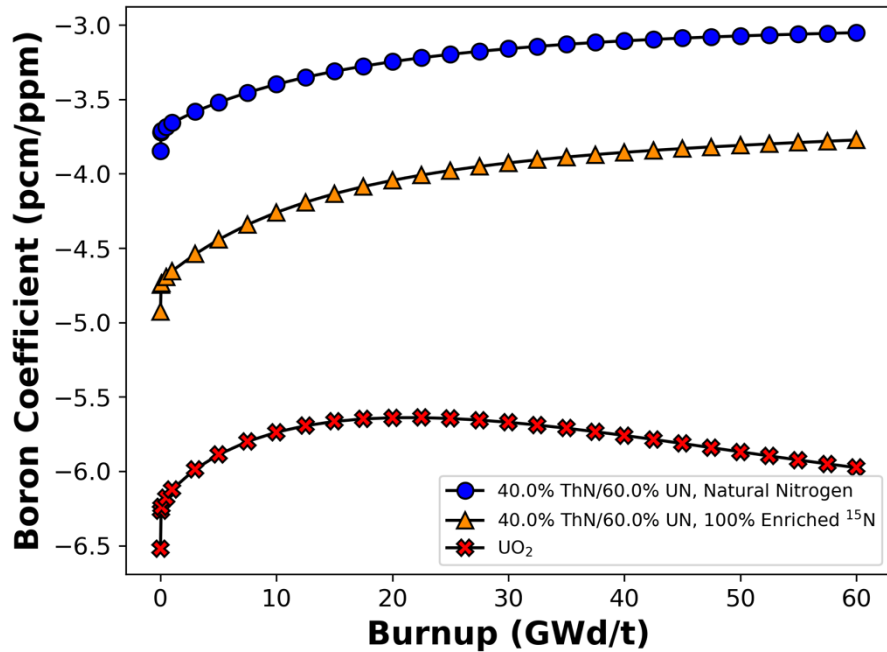


Figure 18: Boron coefficient for UO_2 , 40ThN-60UN with natural nitrogen, and 40ThN-60UN with 100% ^{15}N enrichment

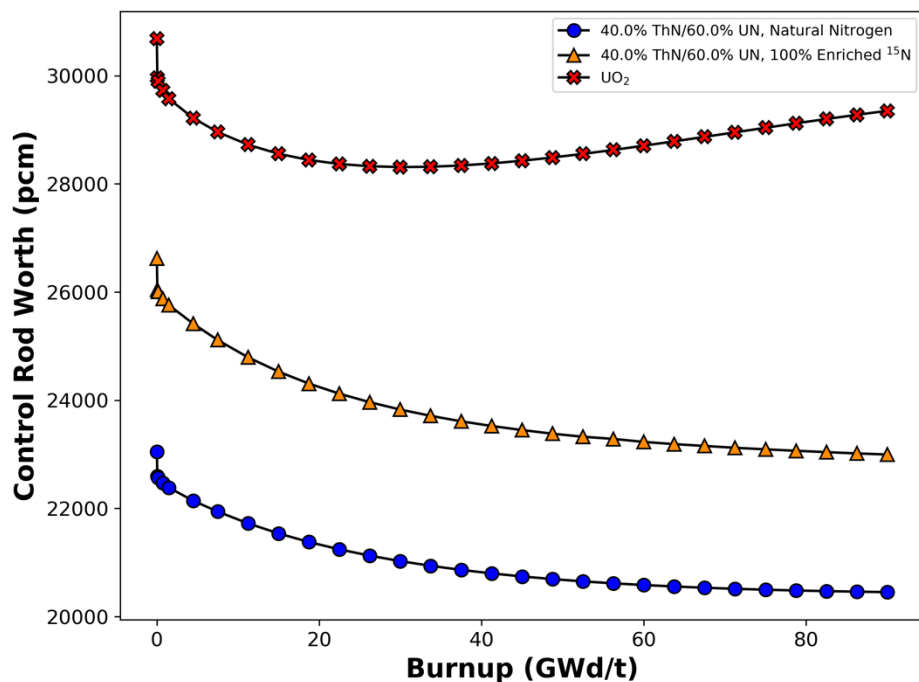


Figure 19: Control rod worth for UO_2 , 40ThN-60UN with natural nitrogen, and 40ThN-60UN with 100% ^{15}N enrichment

There is little difference in Doppler coefficient between the natural nitrogen and enriched ^{15}N cases since this phenomenon is caused by the resonance broadening of the fertile and fissile material (primarily ^{238}U and ^{232}Th). The moderator temperature coefficient is also similar between the natural nitrogen and enriched ^{15}N cases since they both have approximately the same heavy metal loading and therefore the same moderator-to-fuel ratio. By enriching the fuel with ^{15}N , the neutron flux spectrum softens, which increases the worth of soluble boron and the control rods. While the control worth is still not equivalent to that in a UO_2 system, the shutdown margin issue is somewhat mitigated by ^{15}N enrichment.

5. Summary and Conclusions

A preliminary evaluation of mixed ThN-UN fuel forms under normal PWR operating conditions was performed using CASL's neutronics and thermal hydraulics tools MPACT and CTF within the VERA-CS modeling suite. On its own, UN has a higher thermal conductivity and uranium density compared to UO_2 , but it deteriorates in water environments. ThN has an even greater thermal conductivity than UN, but thorium has no fissile isotopes and requires an external neutron source to be transmuted to the fissile ^{233}U . In the proposed fuel form, UN provides the external fissile material needed to transmute ^{232}Th into ^{233}U , while the inclusion of ThN in a UN fuel pellet may reduce the chemical reactivity with water. Further investigation is needed to understand these characteristics.

For any ATF candidate fuel to be considered for real-world application, it must perform equally as well as UO_2 in terms of fuel performance. Because of this requirement, ThN-UN mixtures and ^{235}U enrichments were determined that matched the cycle length of UO_2 . When natural nitrogen is used, the maximum ThN weight fraction obtainable while remaining under the

proliferation limit of 20% ^{235}U enrichment was 66%, with the balance being UN. For a mixture consisting of 40% ThN and 60% UN, the required ^{235}U enrichment was 11.10%, and for a 20% ThN, 80% UN mixture, the required enrichment was 7.80%. Pure UN required a 5.20% ^{235}U enrichment to match the ^{235}U cycle length. ^{15}N enrichment was also considered, and the required ^{235}U enrichments for 20% ThN-80% UN, 40% ThN-60% UN, and UN were 5.90%, 8.50%, and 3.90%, respectively. Each of these enrichments is approximately 25% less than the enrichments needed for natural nitrogen, and the maximum possible weight fraction of ThN at 19.90% ^{235}U enrichment increased from 66.0 to 73.5%.

Because CASL tools are optimized for traditional UO_2 fuels, the 2D pin cell calculations were verified using the continuous energy Monte Carlo code Serpent. It was found that MPACT and Serpent agreed within several hundred pcm across all burnup steps and fuel types, with Serpent predicting a greater multiplication factor at BOL and a smaller multiplication factor at EOL for all fuel types. The differences in multiplication factor calculations may be partially explained by using the ENDF/B-VII.1 cross section library in MPACT and ENDF/B-VII.0 in Serpent. It was also shown that MPACT and Serpent agreed on the mass of ^{232}Th and ^{233}U within 1.2% relative difference throughout the entire cycle.

Reactivity coefficients were calculated for the determined UN and ThN-UN fuel compositions and compared to the UO_2 reactivity coefficients. The Doppler coefficient and moderator temperature coefficient were more negative for the UN and ThN-UN fuels but were still within the acceptable limits provided by the AP1000 DCD. Soluble boron worth for the nitride fuels was found to be less negative than the UO_2 case and was outside the AP1000 limits. Control rod worth was also found to be less for UN and the ThN-UN mixtures, which, in conjunction with the more negative moderator temperature coefficient, may lead to an

insufficient shutdown margin. When 100% enriched ^{15}N was used, the Doppler and moderator temperature coefficients were similar to the natural nitrogen cases. The worth of the soluble boron and control rods increased from using enriched ^{15}N , but they were still less than the control worth in a UO_2 system. Although the reduced control rod worth may partially be compensated for by less excess reactivity and ^{15}N enrichment, full-core analysis should be performed to confirm if shutdown margin is truly an issue for UN or ThN-UN-fueled PWRs. If shutdown margin is insufficient for these fuel types, then design changes such as soluble boron with enriched ^{10}B or B_4C control rods may need to be considered.

The thermal performance of ThN-UN fuel in an AP1000 fuel pin was determined using the coupled neutronics and thermal hydraulics capabilities of MPACT and CTF within VERA-CS. Axial distribution of homologous temperature was found at BOL for each fuel form, and results showed that the maximum homologous temperature for the nitride fuels was approximately 60% of the UO_2 homologous temperature. When burnup was considered, the maximum UO_2 homologous temperature was found to be 0.45, whereas the maximum homologous temperature for UN was approximately 0.23. The homologous temperature never surpassed 0.22 for any of the ThN-UN mixtures. This significant reduction in homologous temperature highlights the benefits of nitride fuels from an ATF perspective: these fuels have a larger thermal safety margin and therefore a smaller chance of melting and releasing fission products.

Overall, the preliminary results from this study point to ThN-UN mixtures being a feasible fuel form in a PWR under normal operating conditions, and they may have advantages from a nonproliferation, waste, natural resource abundance, and accident tolerance viewpoint. For these benefits to be realized, further evaluation is required to address key remaining

challenges, such as shutdown margin, ThN-UN chemical reactivity with water, fuel behavior during irradiation, and fuel safety during accident scenarios.

References

- [1] A. T. Nelson, A. Migdisov, E. Sooby Wood and C. J. Grote, 2018. U₃Si₂ behavior in H₂O environments: Part II, pressurized water with controlled redox chemistry, *J Nucl Mater* 500, pp. 81–91.
- [2] S. L. Hayes, J. K. Thomas and K. L. Peddicord, 1990. Material Property Correlations for Uranium Mononitride: III. Transport Properties, *J Nucl Mater* 171(2-3), pp. 289–299.
- [3] M. Uno, T. Nishi and M. Takano, 2012. Thermodynamic and Thermophysical Properties of the Actinide Nitrides, *Compr Nucl Mater* pp. 61–85.
- [4] N. R. Brown, A. Aronson, M. Todosow, R. Brito and K. J. McClellan, 2014. Neutronics performance of uranium nitride composite fuels in a PWR. *Nucl. Eng Des* 275, pp. 393–407.
- [5] B. J. Jaques, J. Watkins, J. R. Croteau, G. A. Alanko, B. Tyburska-Püschel, M. Meyer, P. Xu, E. J. Lahoda and D. P. Butt, 2015. Synthesis and Sintering of UN-UO₂ Fuel Composites, *J Nucl Mater* 466, pp. 745–754.
- [6] J. H. Yang, D.-J. Kim, K. S. Kim and Y.-H. Koo, 2015. UO₂-UN Composites with Enhanced Uranium Density and Thermal Conductivity, *J Nucl Mater* 465, pp. 509–515.
- [7] J. T. White, A. W. Travis, J. T. Dunwoody and A. T. Nelson, 2017. Fabrication and Thermophysical Property Characterization of UN/U₃Si₂ Composite Fuel Forms, *J Nucl Mater* 495, pp. 463–474.
- [8] N. R. Brown, M. Todosow and A. Cuadra, 2015. Screening of Advanced Cladding Materials and UN-U₃Si₅ Fuel, *J Nucl Mater* 462, pp. 26–42.
- [9] P. Rodriguez and C. V. Sundaram, 1981. Nuclear and Materials Aspects of the Thorium Fuel Cycle, *J Nucl Mater* 100, pp. 227–249.
- [10] International Atomic Energy Agency, 2005. Thorium Fuel Cycle - Potential Benefits and Challenges, IAEA-TECDOC-1450.
- [11] M. Lung and O. Gremm, 1998. Perspectives of the Thorium Fuel Cycle, *Nucl Eng Des* 180, pp. 133–146.
- [12] M. Todosow, A. Galperin, S. Herring, M. Kazimi, T. Downar and A. Morozov, 2005. Use of Thorium in Light Water Reactors," *Nucl Technol* 151(2) pp. 168–176.
- [13] C. S. Pillai and P. Raj, 2000. Thermal conductivity of ThO₂ and Th_{0.98}U_{0.02}O₂, *J Nucl Mater* 277, pp. 116–119.
- [14] K. Bakker, E. Cordfunke, R. Konings and R. Schram, 1997. Critical Evaluation of the Thermal properties of ThO₂ and Th_{1-y}U_yO₂ and a Survey of the Literature Data on Th_{1-y}Pu_yO₂, *J Nucl Mater* 250, pp. 1–12.
- [15] S. S. Parker, J. T. White, P. Hosemann and A. T. Nelson, 2019. Thermophysical properties of thorium mononitride from 298-1700 K, Accepted to *J Nucl Mater*.
- [16] J. H. Yang, K. W. Kang, K. W. Song, C. B. Lee and Y. H. Jung, 2004. Fabrication and Thermal Conductivity of (Th,U)O₂ Pellets, *Nucl Technol* 147(1), pp. 113–119.

- [17] T. R. G. Kutty, K. B. Khan, P. S. Somayajulu, A. K. Sengupta, J. P. Panakkal, A. Kumar and H. S. Kamath, 2008. Development of CAP Process for Fabrication of ThO₂-UO₂ Fuels Part I: Fabrication and Densification Behaviour, *J Nucl Mater* 373, pp. 299–308.
- [18] R. Benz, C. G. Hoffman and G. N. Rupert, 1967. Some Phase Equilibria in the Thorium-Nitrogen System, *J Am Chem Soc* 89(2), pp. 191–197.
- [19] D. Manara, C. Ronchi, M. Sheindlin, M. Lewis and M. Brykin, 2005. Melting of Stoichiometric and Hyperstoichiometric Uranium Dioxide, *J Nucl Mater* 342, pp. 148–163.
- [20] L. Van Brutzel, R. Dingreville and T. J. Bartel, 2015. Nuclear Fuel and Deformation Phenomena, *NEA/NSC/R(2015)5*.
- [21] H. Nickel, H. Nabielek, G. Pott and A. W. Mehner, 2002. Long Time Experience with the Development of HTR Fuel Elements in Germany. *Nucl Eng Des* 217, pp. 141–151.
- [22] L. Mathieu, D. Heuer, R. Brissot, C. Garzenne, C. Le Brun, D. Lecarpentier, E. Liatard, J.-M. Loiseaux, O. Méplan, E. Merle-Lucotte, A. Nuttin, E. Walle and J. Wilson, 2006. The Thorium Molten Salt Reactor: Moving on from the MSBR, *Prog Nucl Energ* 48, pp. 664–679.
- [23] D. Heuer, E. Merle-Lucotte, M. Allibert, M. Brovchenko, V. Ghetta and P. Rubiolo, 2014. Towards the Thorium Fuel Cycle with Molten Salt Fast Reactors, *Ann Nucl Energ* 64, pp. 421–429.
- [24] L. B. Freeman, B. R. Beaudoin, R. A. Frederickson, G. L. Hartfield, H. C. Hecker, S. Milani, W. K. Sarber and W. C. Schick, 1989. Physics Experiments and Lifetime Performance of the Light Water Breeder Reactor, *Nucl Sci Eng* 102(4), pp. 341–364.
- [25] A. Radkowsky and A. Galperin, 1998. The Nonproliferative Light Water Thorium Reactor: A New Approach to Light Water Core Technology, *Nucl Technol* 124 (3), pp. 215–222.
- [26] S. Permana, N. Takaki and H. Sekimoto, 2008. Breeding Capability and Void Reactivity Analysis of Heavy-Water-Cooled Thorium Reactor, *J Nucl Sci Technol* 45(7), pp. 589–600.
- [27] S. Permana, N. Takaki and H. Sekimoto, 2007. Feasible Region of Design Parameters for Water Cooled Thorium Breeder Reactors, *J Nucl Sci Technol* 44(7), pp. 946–957.
- [28] N. R. Brown, J. J. Powers, B. Feng, F. Heidet, N. E. Stauff, G. Zhang, M. Todosow, A. Worrall, J. C. Gehin, T. K. Kim and T. A. Taiwo, 2015. Sustainable Thorium Nuclear Fuel Cycles: A Comparison of Intermediate and Fast Neutron Spectrum Systems, *Nucl Eng and Des* 289, pp. 252–265.
- [29] MPACT Team, 2015. MPACT Theory Manual, Version 2.0.0, Oak Ridge National Laboratory and University of Michigan, CASL-U-2015-0078-000.
- [30] J. Leppänen, 2013. Serpent - a Continuous-energy Monte Carlo Reactor Physics Burnup Calculation Code, VTT Technical Research Centre of Finland.
- [31] R. Salko, A. Wysocki, M. Avramova, A. Toptan, N. Porter, T. Blyth, C. Dances, A. Gomez, C. Jernigan and J. Kelly, CTF Theory Manual, The North Carolina State University.
- [32] M. B. Chadwick, M. Herman, P. Oblozinsky, M. E. Dunn, Y. Danon, A. C. Kahler, D. L. Smith, B. Pritychenko, G. Arbanas, R. Arcilla, R. Brewer, D. A. Brown, R. Capote, A. D. Carlson, Y. S. Cho, H. Derrien, K. Guber, G. M. Hale and S. Hoblit, 2011. ENDF/B-VII.1 Nuclear Data for Science and Technology: Cross Sections, Covariances, Fission Product Yields and Decay Data, *Nucl Data Sheets* 112, pp. 2887–2996.

- [33] Westinghouse Electric Company, 2011. AP1000 Design Control Document Rev. 19,.
- [34] M. J. Driscoll, T. J. Downar and E. E. Pilat, 1990. The Linear Reactivity Model for Nuclear Fuel Management, La Grange Park, Illinois: American Nuclear Society.
- [35] J. Zakova and J. Wallenius, 2012. Fuel Residence Time in BWRs with Nitride Fuels, *Ann Nucl Energ* 47, pp. 182–191.
- [36] M. B. Chadwick, P. Oblozinsky, M. Herman, N. M. Greene, R. D. McKnight, D. L. Smith, P. G. Young, R. E. MacFarlane, G. M. Hale, S. C. Frankle, A. C. Kahler, T. Kawano, R. C. Little, D. G. Madland, P. Moller, R. D. Mosteller, P. R. Page and T, 2006. ENDF/B-VII.0: Next Generation Evaluated Nuclear Data Library for Nuclear Science and Technology, *Nucl Data Sheets* 107, pp. 2931–3060.
- [37] E. Fridman and S. Kliem, Pu Recycling in a Full Th-MOX PWR Core. Part I: Steady State Analysis, *Nucl Eng Des* 241, pp. 193–202.